Electronic Supplementary Material (ESI) for Physical Chemistry Chemical Physics.

Supporting Information

Synthesis of hierarchical mesoporous cerium titanate brannerite and uranyl adsorption properties at pH 3.8

Linggen Kong, Tao Wei, Inna Karatchevtseva, Nicholas Scales

Australian Nuclear Science and Technology Organisation, Lucas Heights, NSW 2234 Australia

Table of Contents

1. Characterization

X-ray diffraction (XRD) patterns were recorded using a PANalytical X'Pert Pro diffractometer (Almelo, The Netherlands) with Cu K_α radiation ($\lambda_{\alpha av}$ = 1.541874 Å) at 45 kV and 40 mA. XRD data were obtained using an angular range of 10–50° (2θ) in a continuous mode with a step size of 0.03° (2θ) with an acquisition time of 2 s per step.

The average crystallite size (L) is estimated from the line broadening of the strongest X-ray diffraction peak using the Scherrer formula:

$$L = \frac{0.9\lambda}{\beta \cdot \cos\theta}$$

Where λ refers to the wavelength of the X-rays, β - the full-width at half-maximum height of the (1 1 0) peak (rad) which is obtained by X'Pert HighScore software, and θ - the diffraction angle, and 0.9 - the shape factor.

Raman spectra were used to investigate the structural evolution of the calcined materials using a Renishaw inVia Raman spectrometer equipped with the Argon ion laser (532 nm) and a Peltier cooled CCD detector (Renishaw plc, Old Town, Gloucestershire, UK) at room temperature. Stokes shifted Raman spectra were collected in the static mode in the range of 100–900 cm^{-1} with a spectral resolution of 1.7 cm^{-1} for the 1800 l/mm grating. On average 20 spectra were collected for each sample. The spot size was approximately 1.5 μm for 50x magnification.

Transmission electron microscopy (TEM) investigation was performed on a JEOL 2200FS (JEOL Ltd., Akishima, Tokyo, Japan) instrument, equipped with a field emission gun (FEG) electron source operated at 200 kV to record selected area electron diffraction patterns (SAED). The specimens were prepared using heavily crushed powders, followed by suspending in ethanol and putting one drop of particle suspension onto a holey carbon coated 100-mesh copper grid.

Scanning electron microscopy (SEM) was used to analyze the microstructures of particle morphology. Samples were examined in a Zeiss Ultra Plus scanning electron microscope (Carl Zeiss NTS GmbH, Oberkochen, Germany) operating at 15 kV. A thin carbon film (~ 5 nm) was deposited onto the particulate surface under vacuum condition.

Surface area, pore volume and pore size were determined using nitrogen sorption analysis at 77 K on Autosorb IQ volumetric adsorption analyzer (Quantachrome Instruments, Boynton Beach, Florida, USA). Samples were outgassed overnight at 300 °C overnight to remove CO_2 and water. The N_2 adsorption-desorption isotherms were interpreted by the IUPAC

classification scheme [1]. ASiQwin software computes the pore size distribution using the methods proposed by non-local density functional theory (NLDFT). The pore size distribution and cumulate pore volume with respect to pore diameter was derived from silica model with cylindrical pores and NLDFT adsorption branch model was selected. The maximum pore width in diameter is cut-off at 77.7 nm for pore volume estimation and pore size distribution plotting. The lower confidence limit of the pore width is 1.022 nm. Specific surface area and pore volume are modelled by both conventional Brunauer–Emmett–Teller (BET) theory and molecular simulation density functional theory (DFT). Although from a scientific point of view the assumptions made in the BET theory do not consider micropore filling, it is still widely accepted by the research community for comparison purposes. DFT, on the other hand, considers the mechanisms of micropore filling as well as of pore condensation, evaporation, and hysteresis in mesopores, and can be employed to calculate a reliable pore size distribution over the complete micropore and mesopore range. In the present work, the specific surface areas derived from NLDFT and the Brunauer-Emmett-Teller (BET) were compared.

Thermo-gravimetric analysis (TGA) was performed to determine surface hydroxyl (OH) density of the prepared materials. A Netzsch STA 449F3 Jupiter (Netzsch-Gerätebau GmbH, Selb, Germany) apparatus was employed, an alumina crucible was used for the experiment and aluminum oxide was used as reference material. The heating profile was set as follows under a nitrogen atmosphere: the materials were stabilized at 25 ºC for 10 min, subjected to a heating ramp rate of 10 ºC min^{-1} to 120 ºC, kept for 30 min isotherm. The materials were then heated to 500 ºC with a heating ramp rate of 20 ºC min^{-1}. The surface hydroxyl group density (D_{OH}, OH nm^{-2}) was calculated based on weight loss (g) between 120 ºC (after 30 min dwelling) and 500 ºC.

An Agilent 7900 inductively coupled plasma mass spectrometer (ICP-MS), fitted with a Micromist® concentric glass nebuliser and Peltier cooled glass spray chamber, was used to conduct the elemental analysis. Standard solutions were prepared by accurately diluting three high purity custom NIST traceable 10 mg L^{-1} multi-element solutions into 3 vol% nitric acid, prepared from high purity nitric acid (Merck) and Milli-Q Water. The supernatants were acidified and diluted into the same 3 vol% nitric acid matrix before analysis. Duplicate samples were conducted for ICP-MS analyses with results expressed as (average ± 3σ, N = 2) for capacity and kinetic studies, and (average ± σ, N = 2) for chemical stability study (σ = standard deviation).

2. Uranyl sorption capacity studies

Table S1 Brannerite powder samples for uranyl sorption analyses.

Sample	Template	$SiO_2/CeTi_2O_6$ weight ratio
Φ12w1-4		1:4
Φ12w1-2	Ludox® HS-30 (Φ = 12.4 nm)	1:2
Φ12w3-4		3:4
Φ8w1-2	Ludox® SM-30 (Φ = 6.8–8.5 nm)	1:2
Φ20w1-2		1:2
Φ20w3-4	Ludox® AS-40 (Φ = 20.3 nm)	3:4

Φ is the average diameter of the colloidal silica, calculated based on surface area.

Caution! Natural uranium was used in these studies and precautions for handling radioactive materials must be followed, including proper worker training and special facilities.

Six samples with different porosity morphologies were selected and pH = 3.8 nitric acid solution was utilized for uranyl sorption capacity studies. At room temperature, 20 mg of power was weighed in 2 mL Eppendorf tubes and uranyl solutions (2 mL) (*V/m* = 100 mL g^{-1}) at various U concentrations of 50, 100, 200, 300, 400, 500, 600, 700 mg L^{-1} were added and then rotated on a rotary suspension mixer (Ratek Pty Ltd, Model: RSM6) set at 30 rpm for 48 h. Subsequently, the tubes were centrifuged with setting at 14680 rpm for 8 min (Eppendorf Centrifuge 5424). 1.5 mL of the supernatants was extracted and analyzed for uranium content by ICP-MS. The experimental data were fitted with the Langmuir model [2,3] as shown in below equation.

$$\frac{C_e}{q_e} = \frac{1}{b \cdot q_{max}} + \frac{C_e}{q_{max}}$$

where q_e (mg g^{-1}) is the amount of uranium adsorbed and C_e (mg L^{-1}) is the equilibrium concentration of uranium remaining in solution after a contact time of 48 h with the metal oxide sorbents; q_{max} is the monolayer capacity and b is the Langmuir constant relating the energy and affinity of the adsorbate interaction with the sorbent; q_e (mg g^{-1}) is related to the adsorption capacity. q_e is calculated based on the C_e value which is determined by ICP-MS. The C_e/q_e (y) versus C_e (x) is plotted, the slope ($1/q_{max}$) and the intercept value ($1/b \cdot q_{max}$) are

obtained by the linear equation, and R^2 is the coefficient of determination. The q_{max} and the bq_{max} are the reciprocal of the slope and the intercept, respectively, and b can be calculated accordingly. The Langmuir model trend line is plotted between q_e (y) and C_e (x) with C_e in the range of 0.01–300 mg L^{-1} and 0.01 or 0.1 mg L^{-1} increment.

3. Uranyl sorption kinetic studies

Table S2 Powder samples for uranyl sorption kinetic studies.

Sample	Template	$SiO_2/CeTi_2O_6$ weight ratio	Uranium C_i (mg L^{-1})
Φ12WR1-4	Ludox® HS-30	1:4	400
Φ12WR1-2		1:2	
Φ12WR3-4		3:4	

Three samples using 12.4 nm diameter template and different template to brannerite weight ratios (1:4, 1:2, 3:4) were selected for kinetic studies. The procedure is similar as that of the capacity study to monitor uranyl uptake (initial U concentrations 400 mg L^{-1}) onto the particles at 0.25, 0.5, 1, 2, 4, 8, 24, 48, 96 h. The data were fitted with a pseudo-second-order kinetic model [4]. The rate of uranyl ions uptake onto the sorbent particles were tested using pH = 3.8 HNO_3 aqueous solution.

Experimental data for the uranyl kinetics sorption studies were fitted with a pseudo second order kinetic model as expressed below.

$$\frac{t}{q_t} = \frac{1}{k_2 \cdot {q_e}^2} + \frac{t}{q_e}$$

where q_t (mg g^{-1}) is the amount of uranium adsorbed at time t (h), q_e (mg g^{-1}) is the equilibrium sorption capacity, k_2 (g mg^{-1} h^{-1}) is the overall pseudo-second-order rate constant and h_0 (mg g^{-1} min^{-1}) is the initial adsorption rate where h_0 (mg g^{-1} h^{-1}) = $k_2 \cdot {q_e}^2$. q_t is calculated based on the C_t value (equilibrium concentration of uranium remaining in solution after a contact time of t) which is determined by ICP-MS. The t/q_t (y) versus t (x) is plotted, the slope ($1/q_e$) and the intercept value ($1/k_2 \cdot {q_e}^2$) are obtained by the linear equation, and R^2 is the coefficient of determination. The q_e and the k_2 can be calculated accordingly. The pseudo second order trend line is plotted between q_t (y) and t (x) with t in the range of 0.01–96 h and 0.01 h increment.

4. Chemical stability studies

20 mg of powder samples were weighed in 2 mL Eppendorf tubes and subsequently 2 mL of HNO_3 solutions at concentrations of 0.01, 0.1, 1, or 2 mol L^{-1} were added. Particle suspensions were agitated in the respective solutions for 48 h on a Rotary Suspension Mixers set at 30 rpm then centrifuged at setting at 14680 rpm for 8 min. The supernatants were collected for analysis using ICP-MS. The percentage element (Na, Si, Ce, Ti) released was calculated according to following equation and the results are shown in Table S3.

$$\%Er = \frac{C_t \times \mathrm{V}}{m} \times 100\%$$

where C_t is the elemental concentration of the supernatant determined by ICP-MS, V is the total liquid volume (2 mL), and m is the sample mass.

Table S3 Percentage of released elements (%*Er*) from powders at different acidic concentrations with 48 h contact time at room temperature[a)].

Sample		0.01 mol L^{-1}	0.1 mol L^{-1}	1 mol L^{-1}	2 mol L^{-1}
Φ12w1-4	Na	0.453±0.059	0.493±0.051	0.498±0.000	0.466±0.003
	Si	0.081±0.002	0.287±0.178	0.248±0.001	0.194±0.005
	Ce	0.055±0.021	0.123±0.011	0.404±0.071	0.580±0.013
	Ti	< 0.002	0.034±0.004	0.391±0.032	0.521±0.013
Φ12w1-2	Na	0.539±0.017	0.565±0.012	0.692±0.111	0.652±0.043
	Si	0.075±0.014	0.183±0.010	0.380±0.102	0.292±0.002
	Ce	0.112±0.006	0.257±0.022	0.608±0.100	0.646±0.033
	Ti	< 0.002	0.032±0.002	0.467±0.080	0.625±0.034
Φ12w3-4	Na	0.735±0.110	0.773±0.028	0.808±0.061	0.877±0.145
	Si	0.114±0.041	0.249±0.040	0.332±0.006	0.218±0.071
	Ce	0.044±0.005	0.117±0.012	0.347±0.022	0.411±0.055
	Ti	< 0.002	0.036±0.007	0.431±0.022	0.643±0.097

[a)]The data are expressed as (average ± σ, N=2) (σ = standard deviation).

5. Surface hydroxyl (OH) determination

Thermogravimetric analysis (TGA) was used to determine OH density of the prepared powders using a method developed by Mueller *et al.* [5]. The heating profile was set as following under a nitrogen atmosphere with flow rate 50 cm^3 min^{-1}: the previous 100 °C dried powders were stabilized at room temperature for 10 min then subjected to a heating ramp of 10 ºC min^{-1} to 120 ºC, dwelled for 30 min. Then the materials were heated to 500 ºC with a heating ramp of 20 ºC min^{-1}. The surface hydroxyl group density (D_{OH}, OH nm^{-2}) was calculated based on weight loss (mg) between 120 ºC and 500 ºC using the following equation.

$$D_{OH} = \alpha \frac{(Wt_{T1} - Wt_{T2})}{Wt_{T1}} \times \frac{2N_A}{SA_{BET} \times MW_{water}}$$

where α = 0.625 (calibration factor), T_1 = 120 ºC and T_2 = 500 ºC, Wt_{T_1} is the sample weight after 30 min dwelling at 120 ºC, Wt_{T_2} is the sample weight at 500 ºC. N_A is Avogadro's number and SA_{BET} (nm^2 g^{-1}) is the BET surface area and MW_{water} is the molecular weight of water. OH content per gram powder was determined by:

$$\text{OH } (g^{-1}) = D_{OH} \text{ x } SA_{BET}$$

Duplicate samples were performed with results expressed as the average.

6. Figures

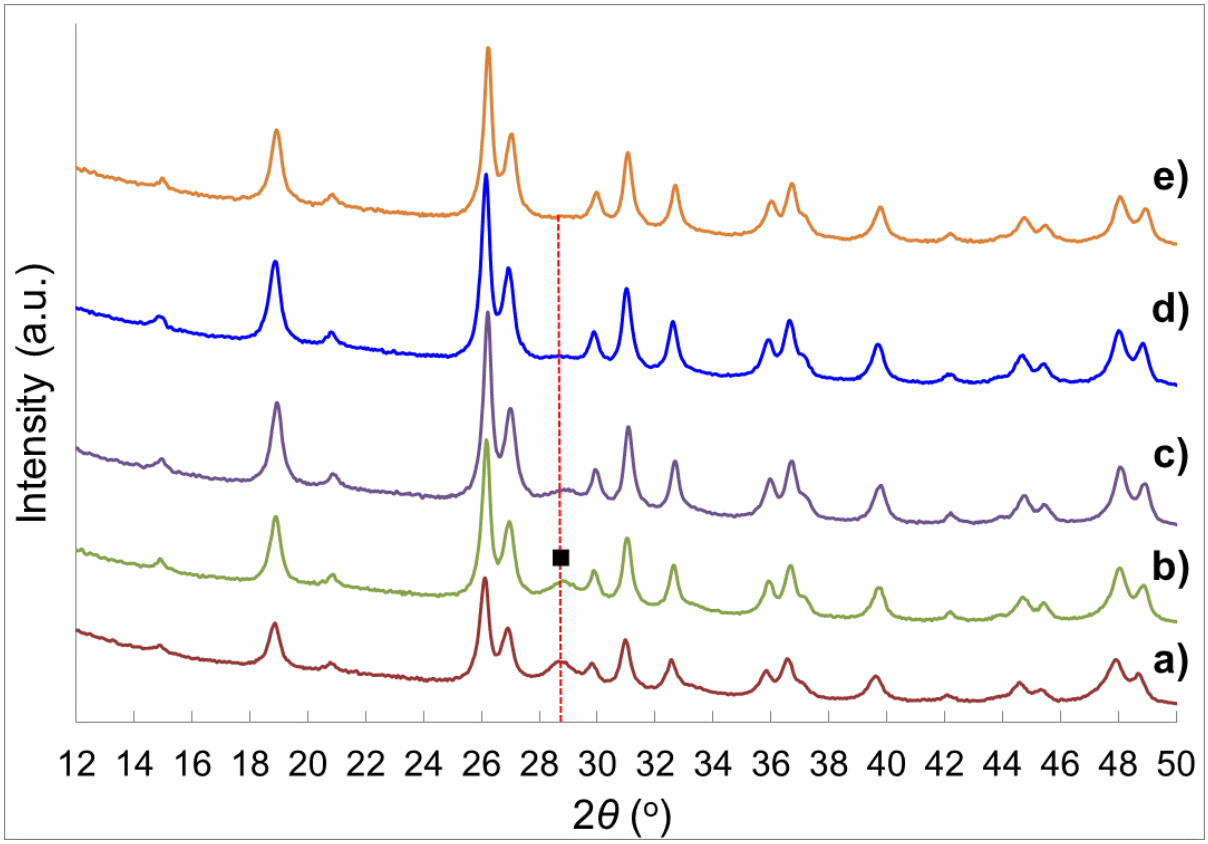

Fig. S1 XRD patterns of brannerite powders calcined at 800 °C for 6 h with composition as a) $CeTi_{2.05}O_6$, b) $CeTi_{2.10}O_6$, c) $CeTi_{2.15}O_6$, d) $CeTi_{2.20}O_6$, e) $CeTi_{2.25}O_6$. Template to brannerite weight ratio is 1:2, (■) CeO_2. Template: 12.4 nm (Φ) colloidal silica.

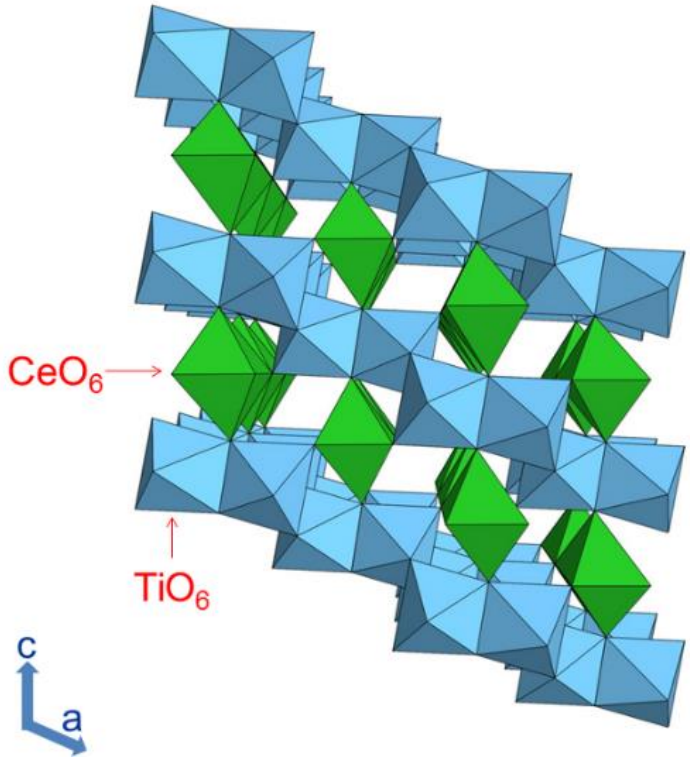

Fig. S2 The $CeTi_2O_6$ brannerite structure viewed along the *b* axis.

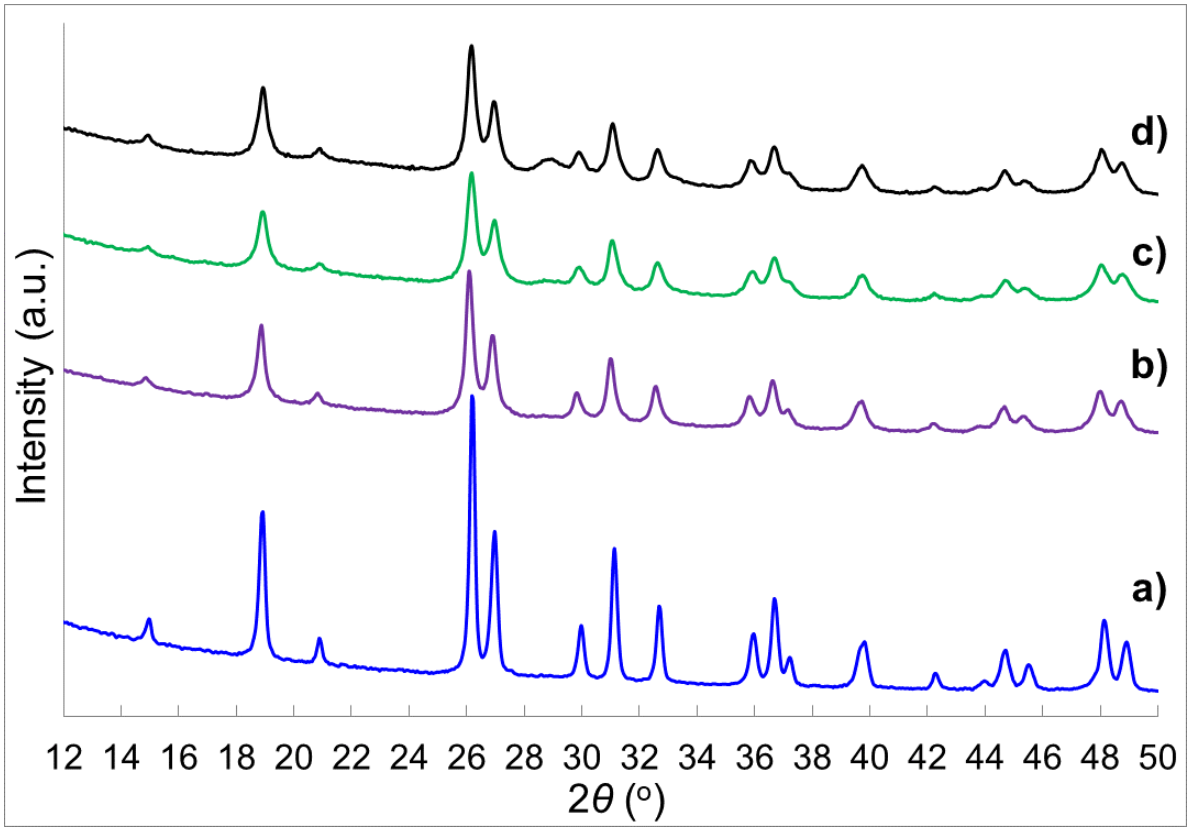

Fig. S3 XRD patterns of brannerite ($CeTi_{2.20}O_6$) powders calcined for 6 h at 800 ºC before leaching 12.4 nm (Φ) colloidal silica. Template to brannerite weight ratio is a) 0, b) 1:4, c) 1:2, d) 3:4.

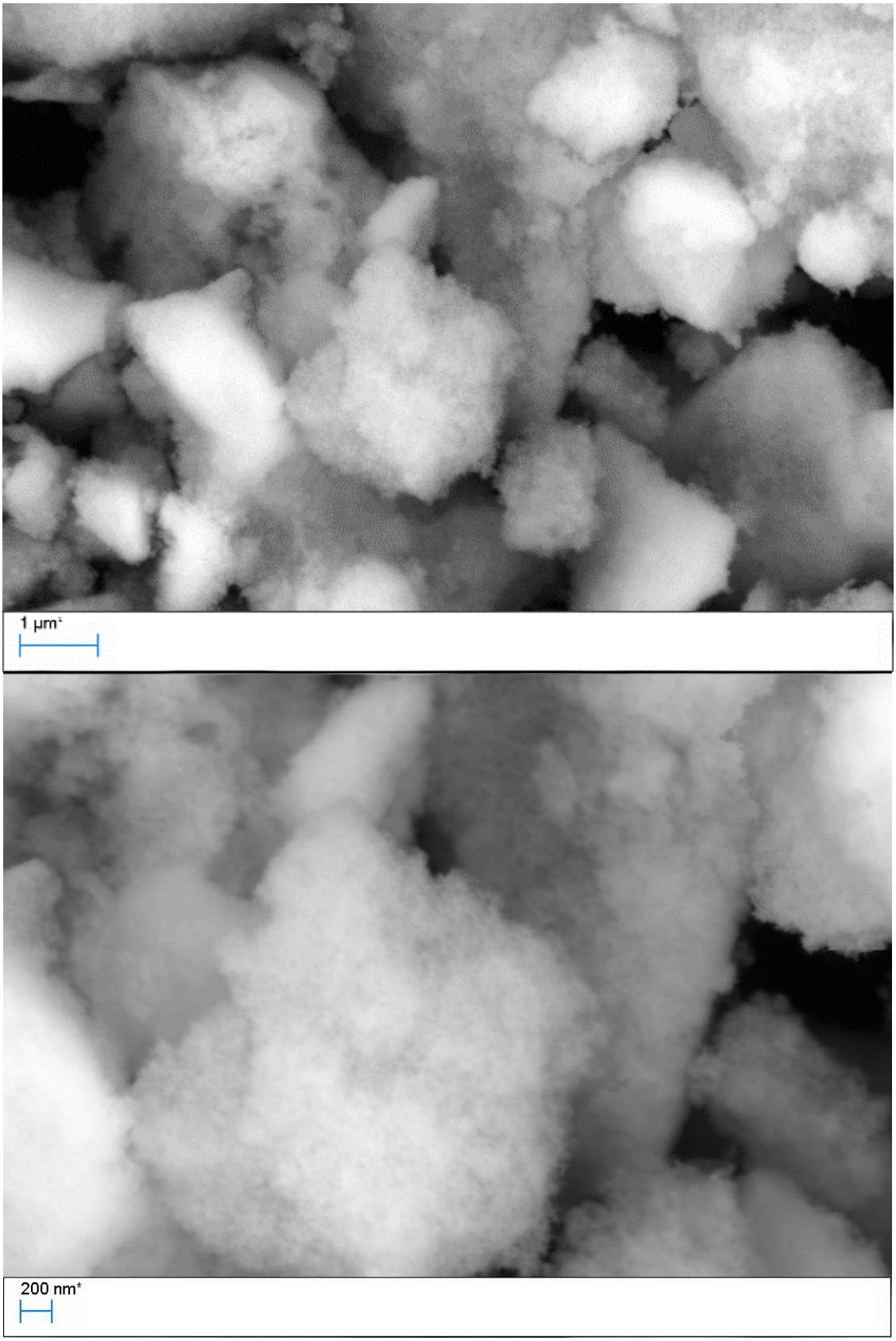

Fig. S4 High magnification SEM images of the brannerite ($CeTi_{2.20}O_6$) particles calcined for 6 h at 800 ºC after leaching 12.4 nm (Φ) colloidal silica with template to brannerite weight ratio being 1:2.

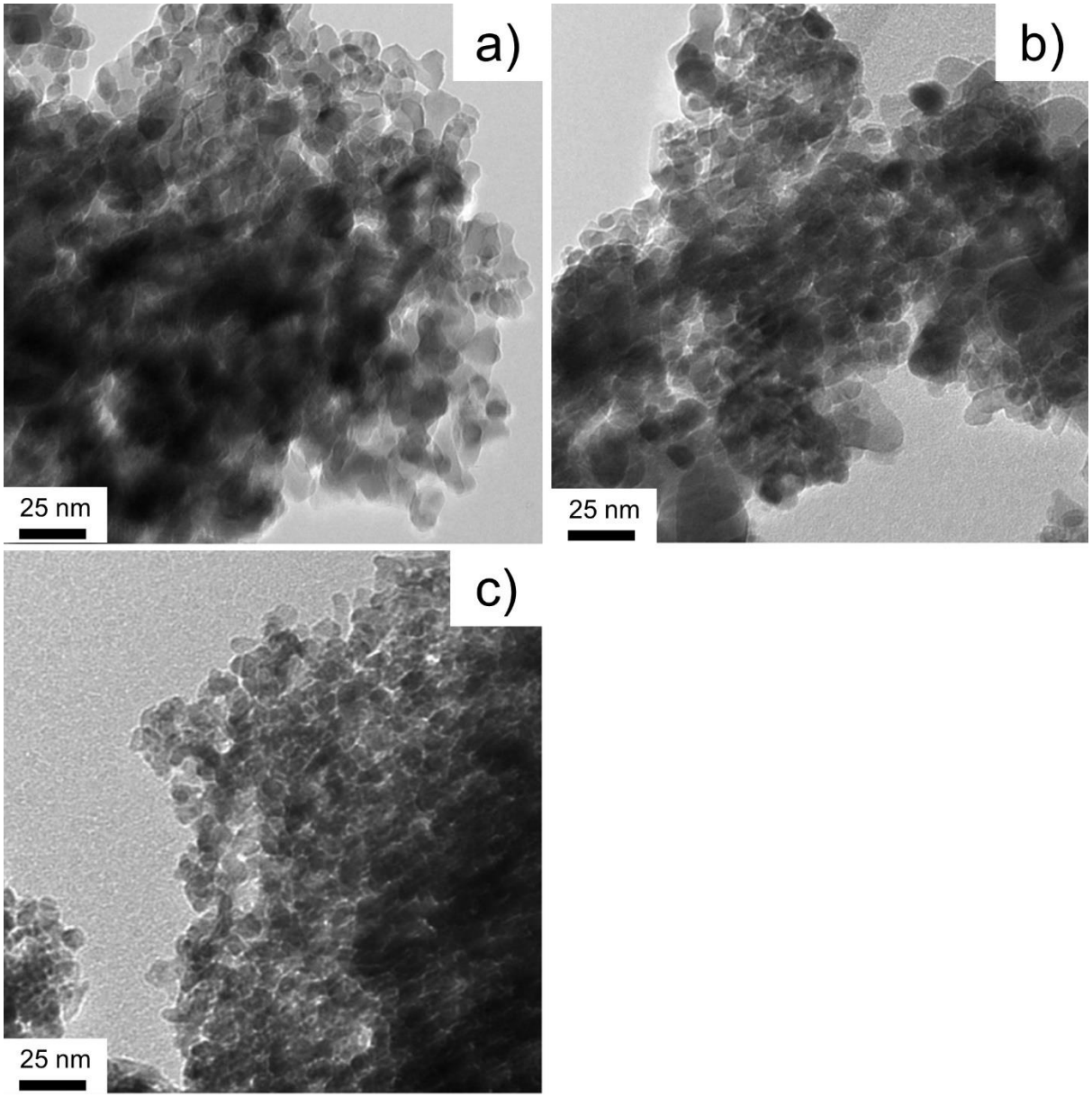

Fig. S5 Bright field TEM images of samples a) Φ12w3-4, b) Φ8w1-2, c) Φ20w1-2.

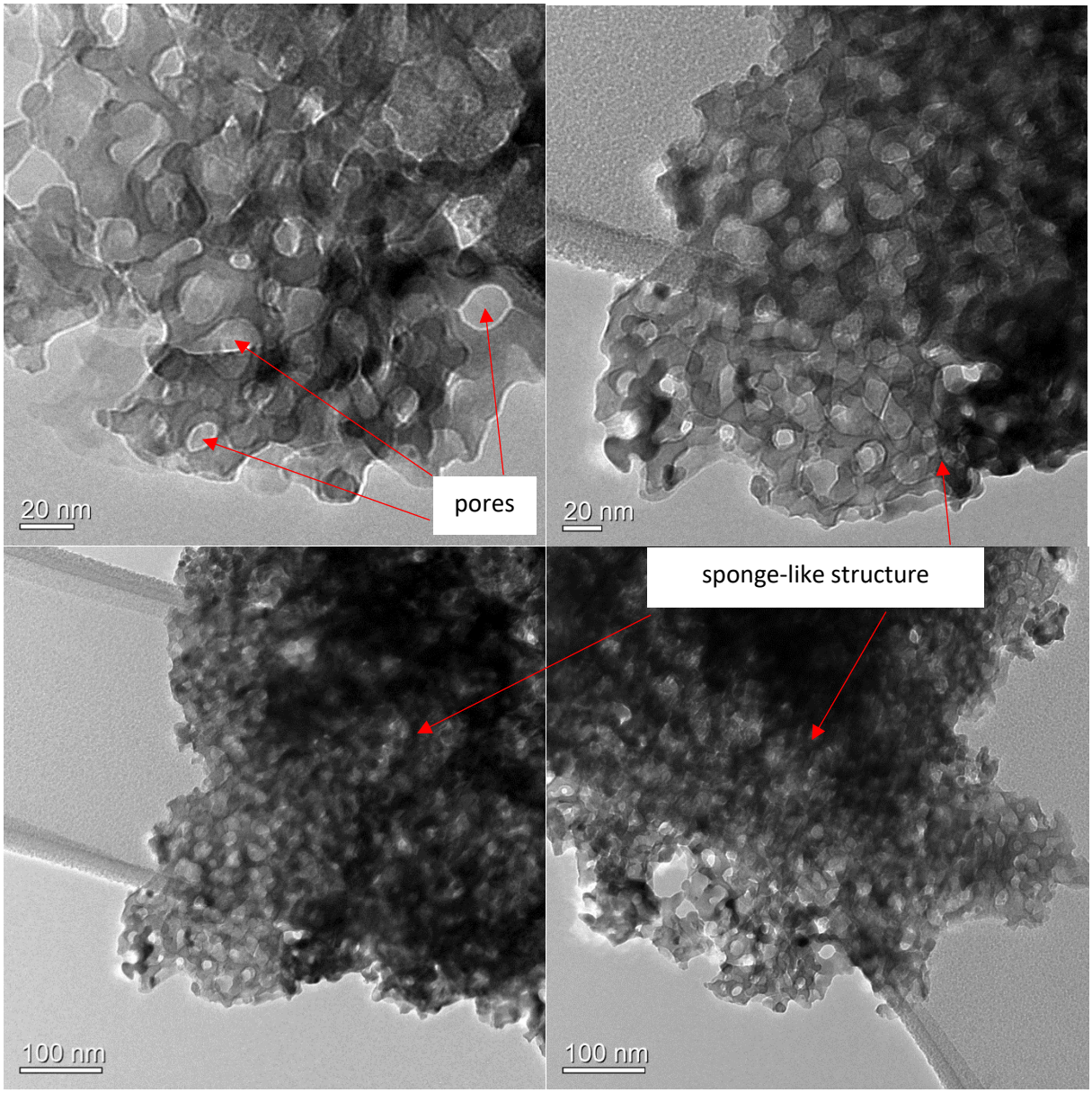

Fig. S6 Bright field TEM images of the brannerite ($CeTi_{2.20}O_6$) particles calcined for 6 h at 800 ^oC after leaching 12.4 nm (Φ) colloidal silica with template to brannerite weight ratio being 1:4.

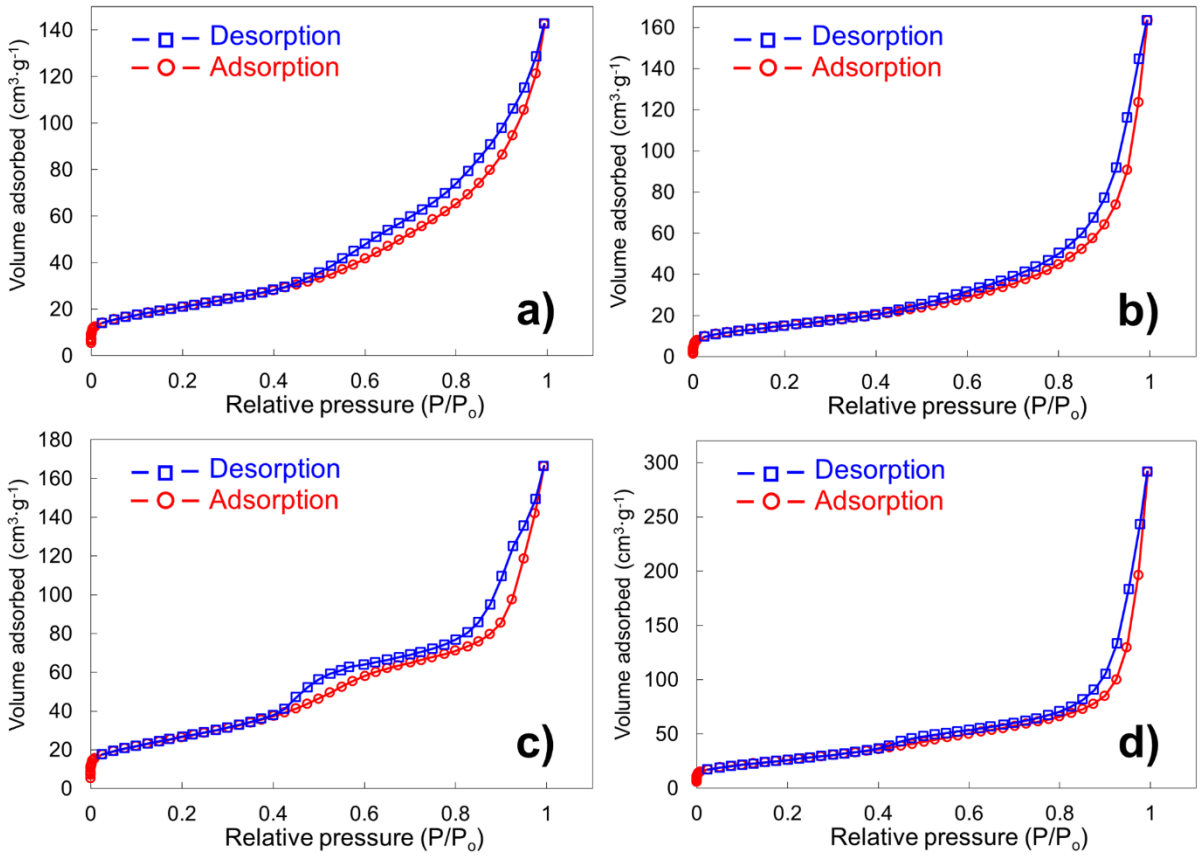

Fig. S7 Nitrogen sorption isotherms for samples a) Φ8w1-2, b) Φ8w3-4, c) Φ20w1-2, d) Φ20w3-4.

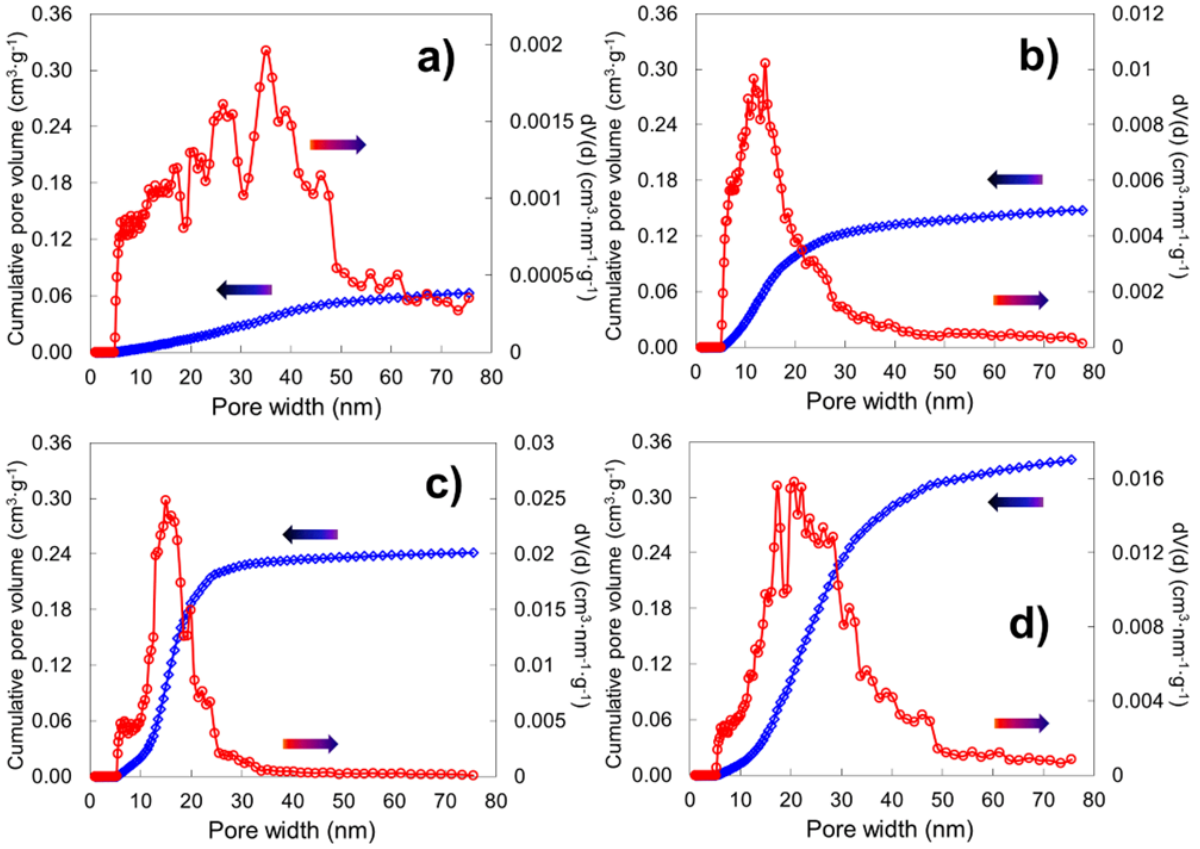

Fig. S8 Pore size distribution and cumulate pore volume with respect to pore diameter by DFT modelling for samples a) w0, b) Φ12w1-4, c) Φ12w1-2, d) Φ12w3-4.

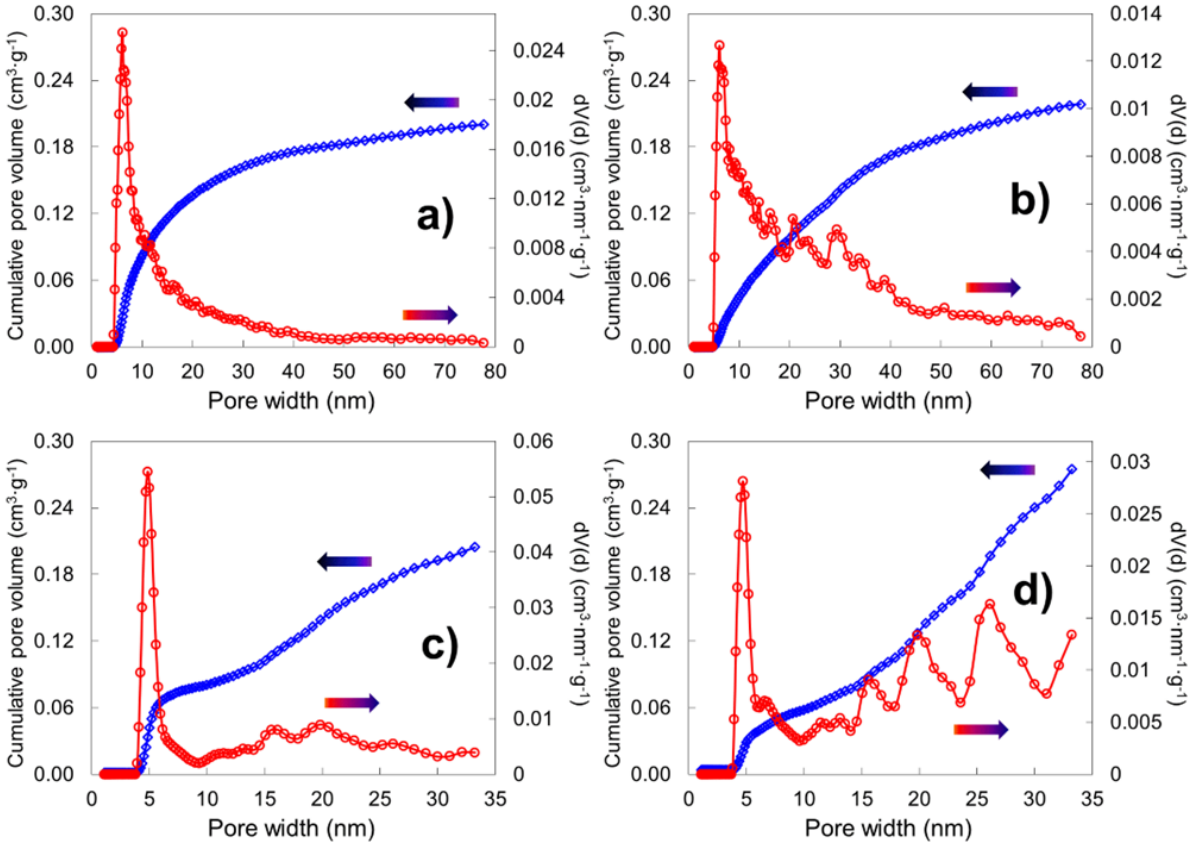

Fig. S9 Pore size distribution and cumulate pore volume with respect to pore diameter by DFT modelling for samples a) Φ8w1-2, b) Φ8w3-4, c) Φ20w1-2, d) Φ20w3-4.

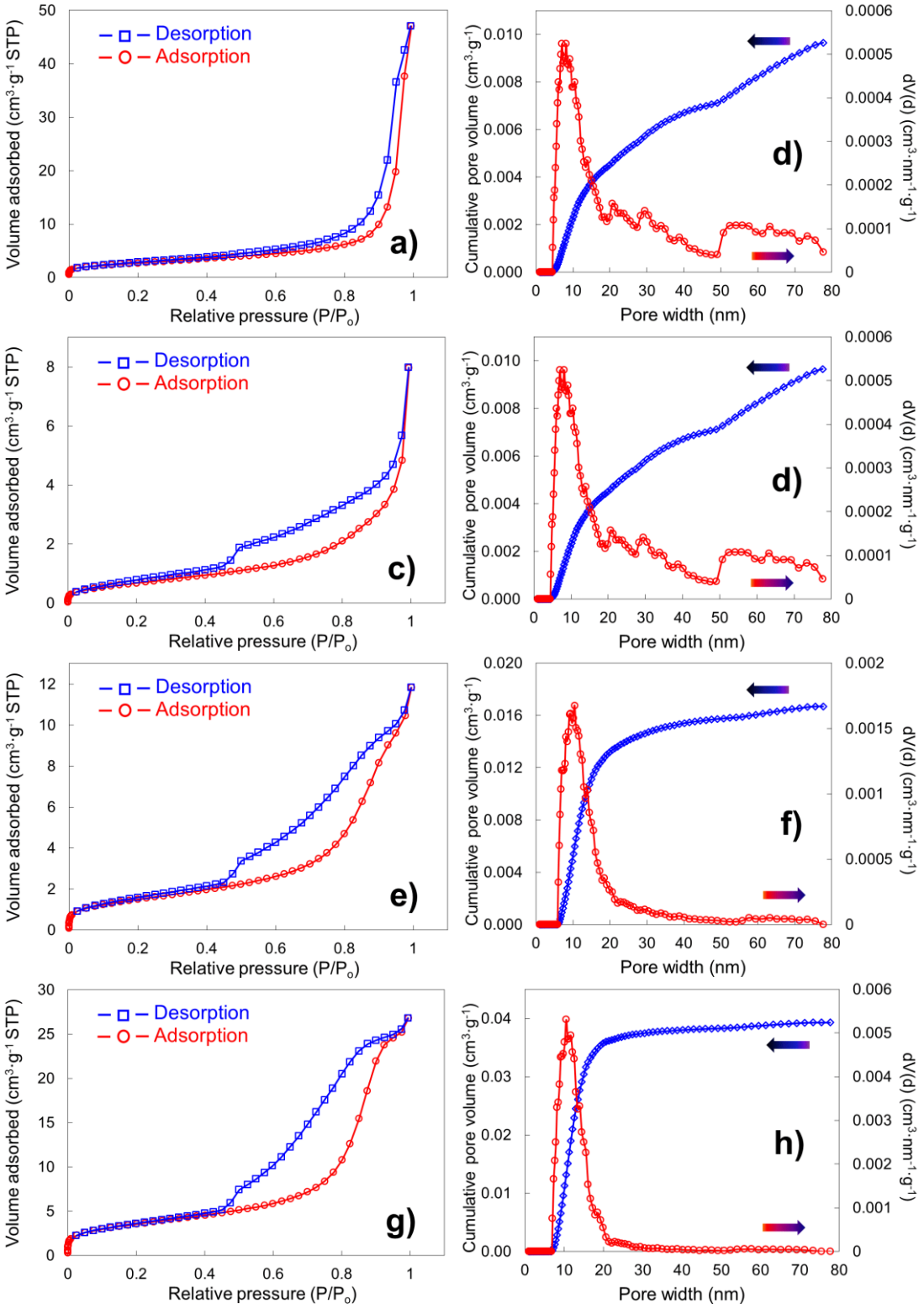

Fig. S10 a, c, e, g) nitrogen adsorption and desorption isotherm, b, d, f, h) the corresponding pore width distribution and cumulate pore volume with respect to pore diameter by DFT modelling for samples a, b) w0, c, d) Φ12w1-4, e, f) Φ12w1-2, g, h) Φ12w3-4. All brannerite ($CeTi_{2.20}O_6$) particles are calcined for 6 h at 800 °C and hard templates are not leached.

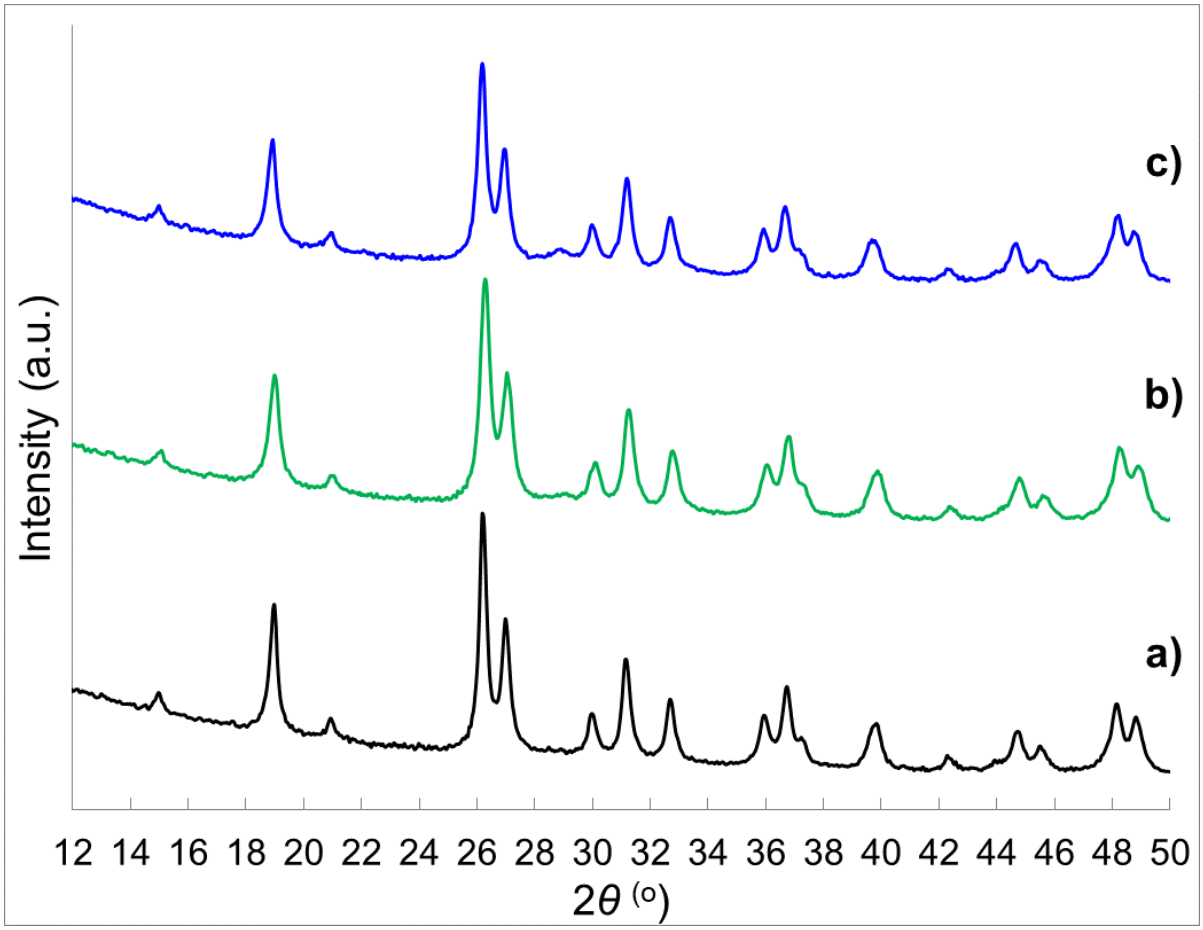

Fig. S11 XRD patterns of template leached brannerite ($CeTi_{2.20}O_6$) powders after immersing in 2 mol L^{-1} HNO_3 solutions for 48 h for samples a) Φ12w1-4, b) Φ12w1-2, c) Φ12w3-4.

7. Tables

Table S4 DFT pore structure data of template leached brannerite powders using 12.4 nm (Φ) colloidal silica at different silica to brannerite weight ratios

Sample	w0	Φ12w1-4	Φ12w1-2	Φ12w3-4
DFT surface area ($m^2\ g^{-1}$)	10.3	40.4	62.8	60.8
DFT pore volume ($cm^3\ g^{-1}$)	0.063	0.148	0.241	0.341
DFT peak pore diameter (nm)	35.0	13.9	15.0	20.6
DFT size < 5 nm (vol%)	0.02	0	0	0
DFT size (5−50 nm) (vol%)	84.8	92.9	98.1	93.2

Table S5 DFT pore structure data of template leached brannerite powders using different colloidal silica (Φ) at different silica to brannerite weight ratios

Sample	Φ8w1-2	Φ8w3-4	Φ20w1-2	Φ20w3-4
DFT surface area ($m^2\ g^{-1}$)	71.6	53.8	94.0	100.1
DFT pore volume ($cm^3\ g^{-1}$)	0.200	0.218	0.205	0.275
DFT peak pore diameter (nm)	6.08	6.08	4.84	4.68
DFT size < 5 nm (vol%)	2.54	0.14	16.3	9.04
DFT size (5−50 nm) (vol%)	89.0	86.6	83.7	91.0

Table S6 Porosity of powders prior to leaching 12.4 nm templates at different silica to brannerite weight ratios

Sample	w0	Φ12w1-4	Φ12w1-2	Φ12w3-4
wt. ratio		1:4	1:2	3:4
mol. ratio	0	1.38:1	2.76:1	4.14:1
vol. ratio		0.57:1	1.13:1	1.70:1
BET surface area ($m^2\ g^{-1}$)	9.85	2.66	5.42	12.8
DFT surface area ($m^2\ g^{-1}$)	9.81	2.41	5.36	13.0
BET pore volume ($cm^3\ g^{-1}$)[a)]	0.073	0.012	0.018	0.041
DFT pore volume ($cm^3\ g^{-1}$)	0.065	0.010	0.017	0.039
Average pore diameter (nm)[b)]	29.6	18.6	13.5	12.9
DFT pore diameter (nm)	29.4	8.15	10.5	10.5
DFT size < 5 nm (vol%)	0	0.59	0	0
DFT size (5−50 nm) (vol%)	89.5	74.7	94.5	97.5

[a)]Single-point total volume of pores at $P/P_0 > 0.99$.

[b)]Average pore diameter determined by BET (4V/A).

wt.: weight; mol.: mole; vol.: volume.

8. References

1 M. Thommes, K. Kaneko, A. V. Neimark, J. P. Olivier, F. Rodriguez-Reinoso, J. Rouquerol and K. S. W. Sing, Physisorption of gases, with special reference to the evaluation of surface area and pore size distribution (IUPAC technical report), *Pure Appl. Chem*., 2015, **87**, 1051–1069. https://doi.org/10.1515/pac-2014-1117

2 I. Langmuir, The constitution and fundamental properties of solids and liquids. Part I solids, *J. Am. Chem. Soc*., 1916, **38**, 2221−2295. https://doi.org/10.1021/ja02268a002

3 M. Chee Kimling, N. Scales, T. L. Hanley and R. A. Caruso, Uranyl-sorption properties of amorphous and crystalline TiO_2/ZrO_2 millimeter-sized hierarchically porous beads, *Environ. Sci. Technol*., 2012, **46**, 7913−7920. https://doi.org/10.1021/es3011157

4 Y. -S. Ho, Review of second-order models for adsorption systems, *J. Hazard. Mater*., 2006, **136**, 681−689. https://doi.org/10.1016/j.jhazmat.2005.12.043

5 R. Mueller, H. K. Kammler, K. Wegner and S. E. Pratsinis, OH surface density of SiO_2 and TiO_2 by thermogravimetric analysis, *Langmuir*, 2003, **19,** 160–165. https://doi.org/10.1021/la025785w

6 L. Kong, D. J. Gregg, I. Karatchevtseva, Z. Zhang, M. G. Blackford, S. C. Middleburgh, G. R. Lumpkin and G. Triani, Novel chemical synthesis and characterization of $CeTi_2O_6$ brannerite, *Inorg. Chem*., 2014, **53**, 6761–6768. http://doi.org/10.1021/ic500563j